Stress History and Effective Shear Strength Parameters Evaluation of a Dilative Stiff Clay

Guilherme H. S. Pinto[1#], *Mariana* Tonini de Araújo[1], *André* O. Faria[1], *Jessé* J. V. Carneiro[1], and *Mauro* P. S. Junior[1].

[1]*Pimenta de Avila Consulting, Geotechnical Engineer, Alameda Oscar Niemeyer, 420 - Sereno Valley, Nova Lima, Brazil*

[#]*Corresponding author: guilherme.henrique@pimentadeavila.com.br*

ABSTRACT

The Cone Penetration Test (CPTu) can be used to evaluate the soil behaviour and properties through correlations (empirical and/or analytical), and the results must be compared to laboratory tests to be validated. This paper presents the evaluation of the effective friction angle (φ') of a stiff over-consolidated Brazilian clay based on CPTu data and laboratory tests characterization, such as index properties, and the comparison of the effective shear strength parameters obtained by triaxial tests. Based on CPTu data, the soil was classified using the Soil-Behaviour Type Classification System (SBTn) proposed by Robertson (2016), and properties such as over-consolidation ratio (OCR) and the effective friction angle were determined using well-known correlations such as Chen & Mayne (1996) and Ouyang & Mayne (2019). The shear response defined by CPTu was compared to the results of isotropic consolidated triaxial compression tests (CIUC). The results showed mainly a clay-like behaviour based on the CPTu data, in agreement with the laboratory characterization, which indicated high plasticity. Regarding the shear response, both the triaxial test and the CPTu data indicated dilative behaviour under shear. Furthermore, the effective friction angle obtained from the triaxial test and the CPTu data were similar depending on the OCR used in the equation, demonstrating the applicability of the adopted methodologies for the Brazilian stiff over-consolidated clay. Finally, based on CPTu data it is proposed a complement of the SBTn developed by Robertson (2016) with OCR isolines.

Keywords: CPTu; soil behaviour; OCR; stiff clay; shear strength

1. Introduction

The piezocone penetration test (CPTu) is commonly used by geotechnical engineering as an efficient, economic, and reliable tool to delineate subsurface stratigraphy, in-situ behaviour, drainage conditions and interpret geoparameters such as strength and stiffness (Robertson, 2009).

The CPTu test can be used to evaluate the soils behaviour since it responds to factors such as stiffness, strength, and compressibility (Robertson, 2016). Thus, the CPTu allows to classify the materials expected behaviour (e.g., clay-like or sand-like behaviours) instead of the textural classifications obtained from laboratory assessment.

When CPTu are performed into clay-like materials in saturated or nearly saturated conditions, at the standard penetration rate, the interpretation traditionally focus on the evaluation of the undrained shear strength (S_u). However, due the stress history, some clay-like materials behave as a dilative material, which makes it necessary to determine the effective shear strength parameters such as effective cohesion (c') and/or the effective friction angle (φ').

Historically, several methodologies were developed to evaluate effective friction angle of sand-like materials as detailed by Roberston & Campanella (1983), Kulhawy & Mayne (1990), Uzielli & Mayne (2019), and others. Nonetheless, for clay-like materials, there is a shortage of approaches in the literature to estimate the effective friction angle (φ'). The methodology proposed by Senneset *et al.* (1989) developed at the Norwegian Institute of Technology (NTH) is the one most widely used in practice.

The original NTH methodology was developed based on undrained penetration of the CPTu test, considering the effective stress limit plasticity solution (Ouyang & Mayne, 2018). In a simplified approach (considering the plastification angle β equal to 0) for normally to lightly-overconsolidated clays and silts (considering c' = 0), the original NTH methodology calculates the effective friction angle considering different porepressure conditions and reaching values between 20º and 40º.

Recently, Ouyang & Mayne (2018) extensively applied the NTH methodology and compared results with laboratory measurements obtained from triaxial compression (TC) tests, either isotropically and/or anisotropically consolidated and undrained shear phase (CIUC, CK0UC, and CAUC). The results obtained by the authors showed the methodology's applicability to different clay types, ranging from soft plastic clays to firm marine clays. In complement, the authors found that the NTH method provides a slightly conservative evaluation of the effective friction angle, reaching lower values compared to the triaxial test.

Also, Ouyang & Mayne (2019) expanded the original NTH methodology to over-consolidated clays, using data from six different databases, such as: (i) laboratory chamber tests in normally consolidated clays; (ii) centrifuge testing in normally consolidated clays; (iii) centrifuge tests in over-consolidated clays; (iv) field CPTu test in natural normally consolidated to lightly over-consolidated clays; (v) field CPTu tests in over-consolidated intact clays with OCR > 2.50; and (vi) field CPTu tests in over-consolidated to fissured clays.

Thus, the intend of this paper is to apply the Ouyang & Mayne (2019) methodology to evaluate the effective friction angle of a Brazilian stiff clay based on CPTu data. The results were compared with those obtained from triaxial tests with isotropic consolidation (CIUC). The in-situ soil behaviour was evaluated using the approach proposed by Robertson (2016) and the drainage condition during the CPTu is discussed based on the approaches suggested by Schneider *et al.* (2008), Schnaid (2009), and Mayne *et al.* (2023). Also, laboratory characterization was performed to fulfil the material database knowledge.

2. Soil Characterization by Grain size Distribution and Atterberg Limits

To evaluate the soil textural classification, 8 samples were collected in different places and depth. The material was characterized by laboratory tests and the main results are shown in Fig. (1) and Fig (2). Considering the mean values, the stiff clay has 48.2% of clay, 17.2% of silt, 32.9% of sand and 1.7% of gravel according to the standard D422-63 (ASTM, 2007).

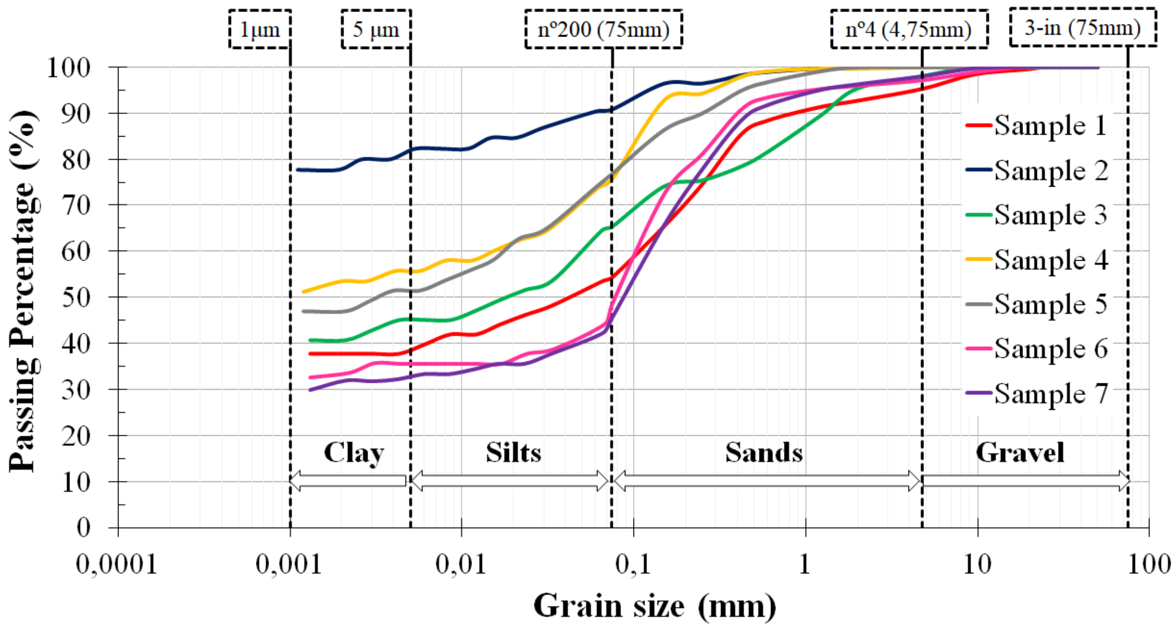

Figure 1. Grain size distribution curves - ASTM D422-63.

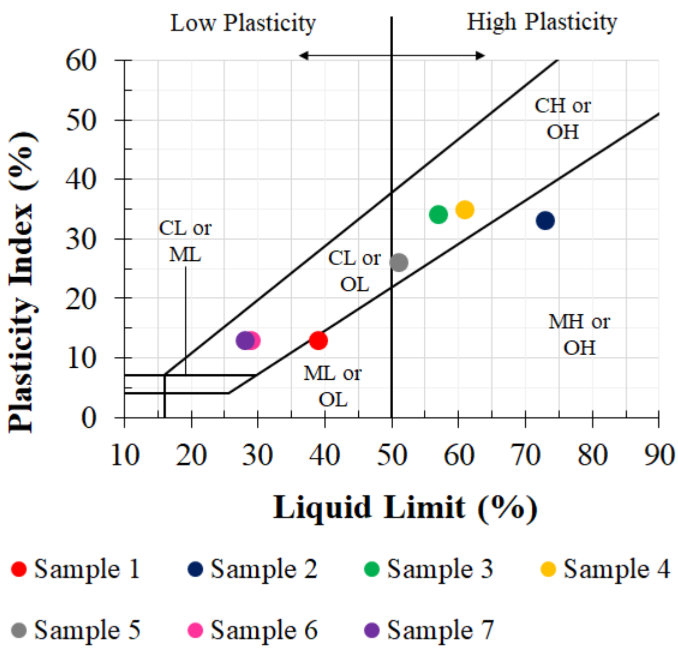

Figure 2. Plasticity chart by laboratory tests – ASTM D4318-17e1.

The Atterberg Limits are shown in Fig. (2), according to standard D4318-17e1 (ASTM, 2018). The mean value of the Limit Liquid (LL) is equal to 48.1% and the Plasticity Index (PI) equal to 23.9%, classifying the material as highly plastic (above the A-line). Finally, the mean value of the specific gravity (ρ_s) is equal to 2.670 g/cm³ according to standard ASTM D792-20 (ASTM, 2020).

3. In situ Behaviour

To evaluate the Brazilian stiff clay in-situ behaviour, 28 CPTus were performed. The CPTus with dissipation tests followed international standard ISO 22476-1 (ISO, 2022) using a 10cm² cone pushed at 2.0 ± 0.5 cm/s with readings taken at every 5 cm. The CPTu performed with dissipation tests provide four independent parameters: (i) the cone tip resistance (q_c), which characterizes the soil resistance to cone penetration; (ii) the sleeve friction (f_s), which represents the soil adhesion to the friction sleeve; (iii) the porewater pressure (u), commonly measured behind the cone tip (u_2 location); and (iv) the equilibrium in-situ porewater pressure (u_0) obtained by the full stop of the cone penetration and the dissipation of the excess porewater pressure. Also, the measured cone resistance was corrected to total cone resistance (q_t) to account for the unequal end area effect using the equation $q_t = q_c + u_2 (1 - a)$, where the "a" value is around 0.80 (Lunne *et al.*, 1997).

As detailed by Robertson (2016), the normalized parameters are more consistent and reliable to evaluate the in-situ soil behaviour. Based on this, the author uses the normalized porepressure (Eq. 1), the normalized Friction Ratio (Eq. 2) and the normalized cone resistance (Eq. 3) to evaluate the in-situ behaviour.

$$B_q = \frac{u_2 - u_0}{q_t - \sigma_{v0}} \qquad (1)$$

$$F_R = \frac{f_s}{q_t - \sigma_{v0}} \; x \; 100\% \qquad (2)$$

$$Q_{tn} = \left(\frac{q_t - \sigma_{v0}}{Pa}\right)\left(\frac{P_a}{\sigma'_{v0}}\right)^n \qquad (3)$$

Where σ_{v0} is the total vertical stress and Pa is the atmospheric pressure, and the exponent "n" is a function of soil type (usually equals to 1 to clay-like materials) as detailed by Robertson (2016).

Figure 3 and 4 summarizes the 28 CPTus in which was observed the stiff clay. As observed in Fig. (3), q_t varies from 2,000 kPa to 10,000 kPa with the mean value around 6,000 kPa approximately. It was not observed any pattern in the f_s, but a dispersion of the measured values. In Fig. (4) is presented the normalized parameters, where it is noted that the Q_{tn} varies between 10 to 60 and that the F_r mean value is around 6% as expected to clayey materials (Mayne *et al.* 2023).

The dissipation tests showed an equilibrium porepressure (u_0) almost equals to a 100% hydrostatic in all CPTus analysed. It is important to emphasize that most of the dissipation tests were performed in a saturated or nearly saturated condition, since the material is located under the phreatic surface according to monitoring instruments.

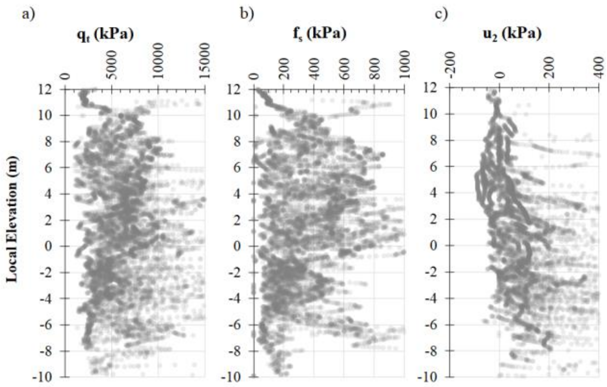

Figure 3. CPTu basics parameters: a) q_t; b) f_s; and c) u_2.

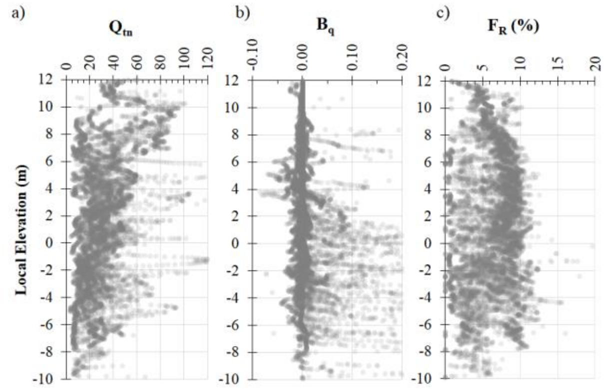

Figure 4. CPTu normalized parameters: a) Q_{tn}; b) B_q; and c) F_r.

In general, the material does not generate considerable excess porewater pressure, as can be seen by the B_q in Fig. (4) with the values almost equal to 0 in all the CPTu profile. Since B_q does not reach the interval of 0.30 to 0.50, as suggest by Schnaid (2009) for undrained penetration, possibly the CPTus tests were performed in a partially drained or drained condition. This condition will be further explored using the chart proposed by Schneider *et al.* (2018) and the I_Q-B_q index proposed by Mayne *et al.* (2023).

Figure 5 shows two typical dissipation tests performed in the stiff clay. It is noted that the porewater pressure increases over time due to negative excess porepressure generated during the penetration (values increasing to an equilibrium condition). The induced negative shear porepressure was dissipated at the end of the shear solicitation promoted by the cone penetration. This behaviour is commonly observed in dilative materials due to the high excess porewater pressure generated at the cone tip (u_1 location) and low excess porewater pressure behind the cone (u_2 location) as demonstrated empirically by Robertson *et al.* (1986) Lunne *et al.* (1997) and numerically by Song *et. al* (2019).

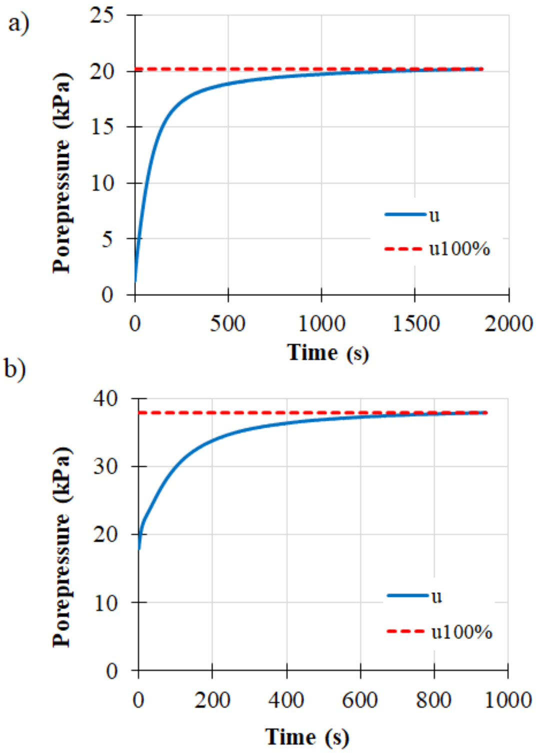

Figure 5. Dissipation Tests at different elevations: a) 9.1 m; and b) 18.9 m.

In addition to the initial evaluation, the soil behaviour chart proposed by Roberson (2016) was applied. As described by the author, the in-situ soil behaviour is controlled by stiffness, strength and compressibility. Based on this, the author proposed the Soil Behaviour Type Classification System (SBTn) to classify different non-structured geomaterials, based on its in-situ behaviour using the CPTu.

Roberson (2016) introduced a modified soil behaviour type index, I_B, which classifies the soils in three major groups: (i) for $I_B < 22$ the materials are classified as clay-like soils; (ii) for $22 < I_B < 32$ the materials are classified as transitional (silts in general); and (iii) for $I_B > 32$ the materials are classified as sand-like behaviour. The I_B can be calculated using the Eq. (4).

$$I_B = \frac{100(Q_{tn}+10)}{(Q_{tn}F_R+70)} \quad (4)$$

Also, the author introduced the Contractive/Dilative boundary (CD) to classify different soils based on its dilatancy. CD values higher than 70 indicate dilative response at large strain and values lower than 70 indicate contractive behaviour at large strains. The CD boundary combines two different criteria: i) $Q_{tn,cs} = 70$ for sand-like soils (state parameter equals to -0.05); and ii) OCR = 4 for transitional and clay-like soils. This contour can be calculated using Eq. (5).

$$CD = 70 = (Q_{tn} - 11)(1 + 0{,}06F_R)^{17} \quad (5)$$

In addition to the SBTn proposed by Roberston (2016), for the present paper the OCR isolines were constructed using Eq. (6), proposed by Chen & Mayne (1996), within the OCR range of 2 to 20. To validate the isolines proposed, OCR equals to 4 (red line in Figure 6) was compared to the original CD boundary equals to 70, as suggested by Robertson (2016).

$$OCR = 0.317\left(\frac{q_t - \sigma_{v0}}{\sigma'_{v0}}\right) \quad (6)$$

Figure 6 shows the SBTn results and OCR isolines considering all the CPTu data of the analysed stiff clay. It is noted that almost all the data presents clay-like behaviour (≈ 98% of the data) and a dilative response at large strains (≈ 87% of the data), since most of the points plot above the CD = 70 boundary and almost all data are below the I_B boundary of 22. Also, is noted an agreement of the isolines and the Robertson (2016) boundary.

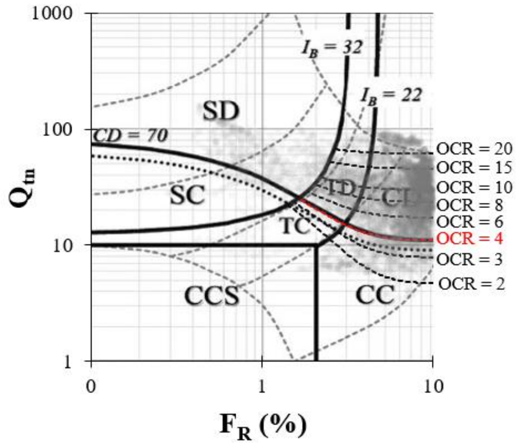

Figure 6. SBTn chart proposed by Robertson (2016) with OCR's isolines and the data of the CPTu test performed in the stiff clay.

In complement to the SBTn, the in-situ drainage conditions were initially accessed using the B_q values and then evaluated by the methodology proposed by Schneider *et al.* (2008). Figure 7 shows the results of this evaluation and, as can be seen, the material has a drained/partial drained condition, since data plots in the sand-like (drained condition) and transitional-contractive (partial drained condition) regions. These results indicate that the stiff clay analysed has a dilative response and the evaluation of the undrained shear strength may not be applicable. It is important to mention that the chart proposed by Schneider *et al.* (2008) has different classifications than Robertson (2016) and Fig. (7) was used only to evaluate the drainage conditions.

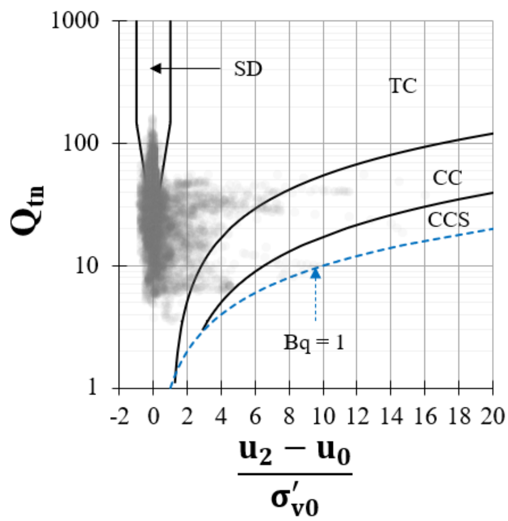

Figure 7. Drainage conditions of the stiff clay according to the Schneider *et al.* (2008) methodology.

The assessment of the drainage condition was further complemented with the I_Q-B_q index proposed by Mayne *et al.* (2023). As described by the author, the parameter I_Q-B_q values higher than 4 indicate a drained or partially drained condition. Figure 8 shows the result obtained, where the majority of the data indicates a drained/partially drained penetration. Based on this, the undrained shear strength of the material was not determined using the CPTu, and the focus was the evaluation of the effective friction angle (φ').

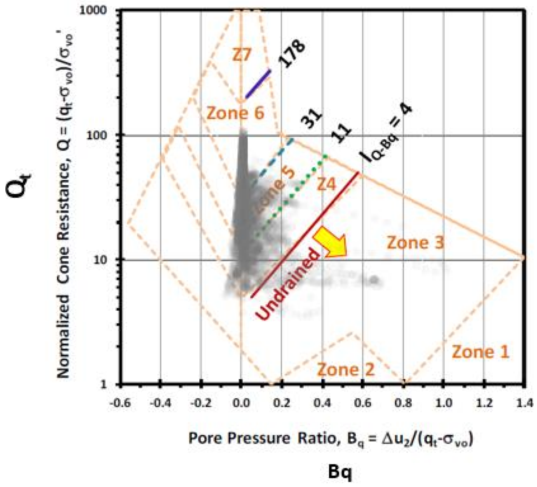

Figure 8. Drainage conditions of the stiff clay using the I_Q-B_q index (Adapted from Mayne *et al.*, 2023).

Since the stiff clay shown herein is in a saturated and dilative state, it is paramount to determine its effective friction angle, which will be discussed in the next pages.

4. Effective Shear Strength

The effective shear strength parameters were determined based on laboratory tests using three triaxial compression tests with isotropic consolidation and undrained shearing (CIUC) performed in undisturbed samples. The tests applied confining pressures equal to 100 kPa, 200 kPa, 400 kPa and 800 kPa and followed the procedures described by ASTM D4767-11 (ASTM, 2020). Subsequent analyses were performed to compare the results with the effective friction angle obtained using the Ouyang & Mayne (2019) methodology based on CPTu data applying the expanded NTH methodology.

4.1. Triaxial Compression Tests

Figure 9 shows the triaxial compression tests interpretation and the effective shear strength parameters evaluation. The deviator stress mainly shows a ductile behaviour without any expressive shear strength reduction over the axial deformation (except Test 2 with confining pressure of 800 kPa).

In the same figure it is possible to note that the soil has a tendency to contract (generates a positive excess porewater pressure) until an axial deformation of 1% to 2% when the tendency to dilation starts and the porewater pressure starts to decrease with further deformation.

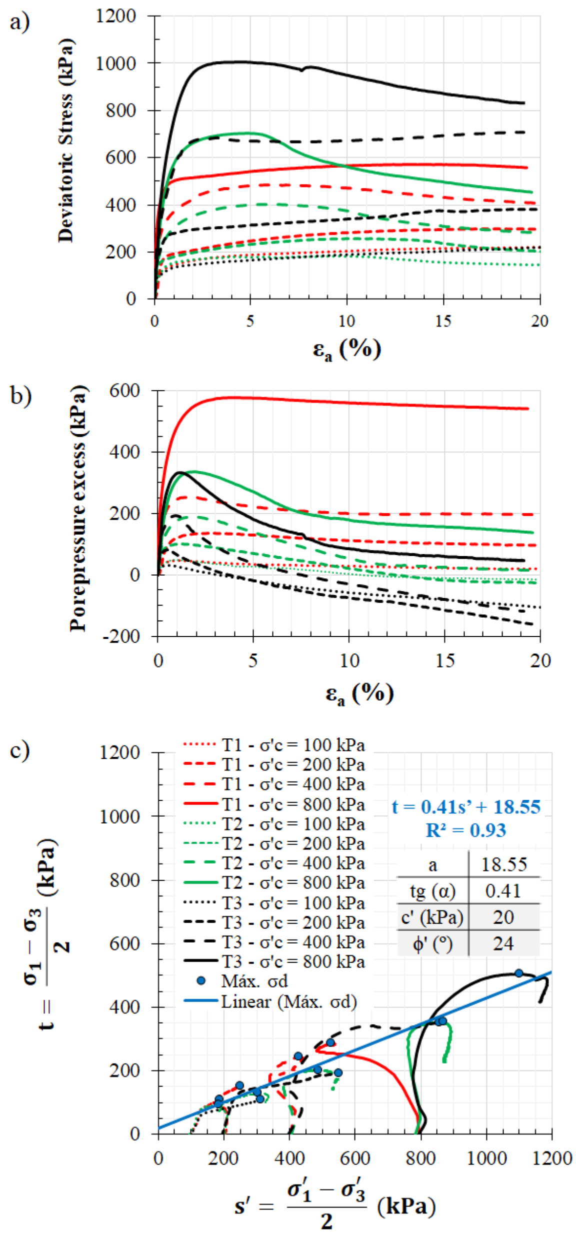

Figure 9. Triaxial Compression Tests (CIUC) interpretation: a) deviator stress *x* axial strain; b) excess porewater pressure *x* axial strain; and c) effective stress path and effective shear strength parameters.

Using the maximum deviator stress criteria (Lade, 2016), the effective shear strength parameters were calculated for all samples. Based on this, it was obtained an effective cohesion of 20 kPa (c'_{txc} = 20 kPa) and effective friction angle of 24º (φ'_{txc} = 24º).

The final failure plane of the stiff clay in the triaxial compression test apparatus is depicted in Fig. (10). As can be seen, Test 2 and Test 3 samples formed a shear band failure plane, consistent with the stiff behaviour (Castro, 1969), the porewater pressure obtained from the triaxial compression test and the in-situ dissipation test performed during the CPTu test.

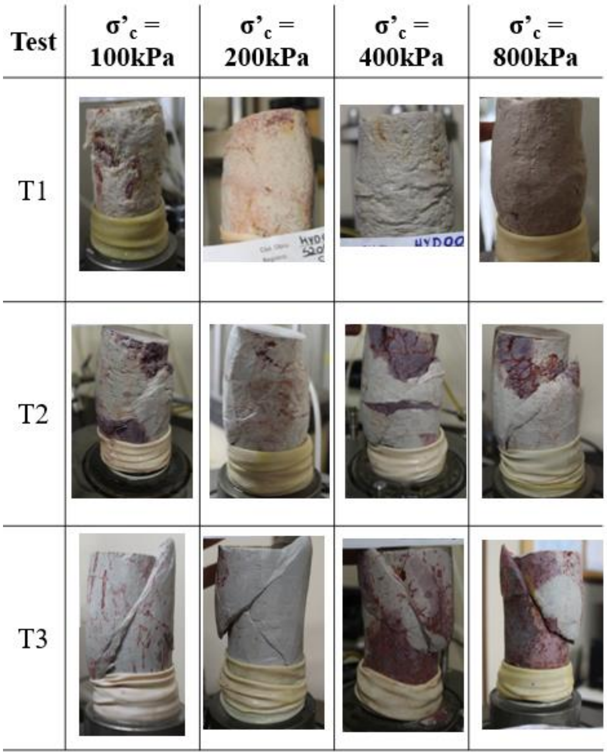

Figure 10. Pictures of the samples at the end of the triaxial tests.

4.2. Strength Parameters determined using the CPTus tests

To evaluate the effective friction angle (φ') of normally consolidated to fissured clays, Ouyang & Mayne (2019) propose the Eq. (7) and Eq. (8), which are an expansion of the NTH solution (Senneset *et al.*, 1989) originally develop for normally consolidated clays.

$$\varphi' = 29.5.B_q^{\ 0,121}\left[0.256 + 0.336Bq + log\frac{q_t-\sigma_{v0}}{(\sigma'_{v0}OCR^{\lambda})}\right] \quad (7)$$

valid to: $0.05 < \mathrm{B_q} < 1.00$.

$$\varphi' = 8.18ln\left[2.13\frac{q_t-\sigma_{v0}}{(\sigma'_{v0}OCR^{\lambda})}\right] \quad (8)$$

valid to: $\mathrm{B_q} < 0.05$.

Where λ is the stress exponent and approximately equals to $1 - C_c/C_r$, where C_c is the virgin compression index and C_r is the recompression index as detailed by Ouyang & Mayne (2019). The exponent λ can be determined using the oedometer tests or estimated as 0.80±0.10 for natural and intact clays, as detailed by Mayne *et al.* (2023). Also, the results of Eq. (7) and Eq. (8) are valid for effective friction angle between 15º and 45º, following the validation presented by Ouyang & Mayne (2018, 2019).

Equation (6) was used to evaluate the stress history of the stiff-clay and it was selected a value of OCR = 4 to use in the equation proposed by Ouyang & Mayne (2019) to determine the effective friction angle. The OCR isolines with the date determined from the CPTu tests are shown in Fig. (6) with the boundary OCR = 4 highlighted in red. Also, since the CPTu is not applicable to evaluate effective cohesion, this value was assumed equals to zero to apply the equations proposed by Ouyang & Mayne (2019).

Using the exponent equal to 0.70 (λ = 0.70), such as the values adopted by Ouyang & Mayne (2019) to regular and intact clays, the effective friction angle was calculated and plotted in the histogram and boxplot showed in Fig. (11). Also, in the same figure a normal distribution curve was adjusted based on data obtained. This distribution was chosen as expected distribution to effective friction angle as shown by Assis (2020). Also, it is noted that the normal curve seems to agree with histogram data.

The mean value obtained was approximately 26º with a standard deviation equals to 5º. Based on this data the Coefficient of Variation (C.V.), defined as the standard deviation divided by the mean value, was equal to 18.1%. The C.V. found is slightly higher than that found by Assis (2020), who observed values between 5% and 15% for effective friction angle. This higher scatter can be caused by some variance in measurements of the CPTu, such as the q_t and u_2, the OCR estimation by the methodology applied and other factors such as the mineralogy, the natural uncertainty of the applied methodology and the natural scatter of the effective friction angle (Ouyang & Mayne, 2018).

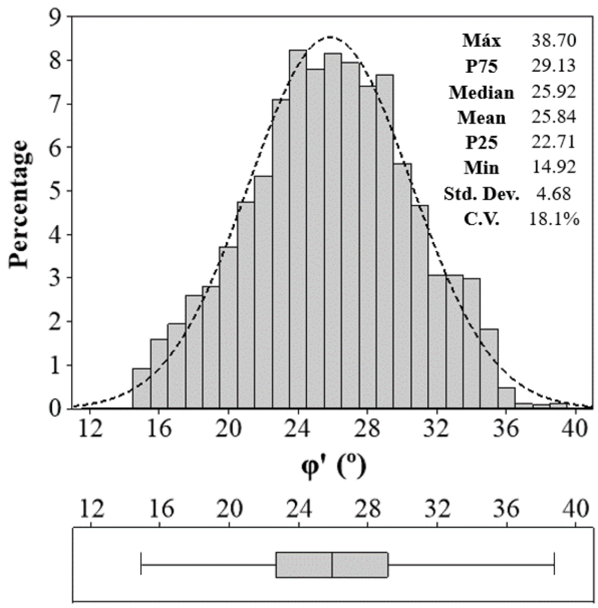

Figure 11. Histogram and boxplot of the effective friction angle with OCR = 4 and λ = 0.70.

4.3. In situ and laboratory determination of the effective friction angle

The friction angle obtained by the triaxial test (φ'_{txc} = 24º) was used to evaluate the representative percentile of the friction angle distribution calculated by the CPTu test (Fig. (11)). Figure 12 shows that the 35th percentile of the CPTu distribution corresponds to the value obtained for the triaxial interpretation. Comparing this result with Ouyang & Mayne (2018), 65% of the in-situ data has higher values than that obtained for the triaxial test when applying the modified NTH methodology.

Analysing the mean values obtained by field and laboratory assessment (φ'_{CPTu} = 26º and φ'_{txc} = 24º) the difference observed is lower than one standard deviation (5º). However, the difference observed by the methodologies (2.0º) is the same range of variation observed by Ouyang & Mayne (2019), which was 1.5º comparing the triaxial test result with the CPTu methodology prediction.

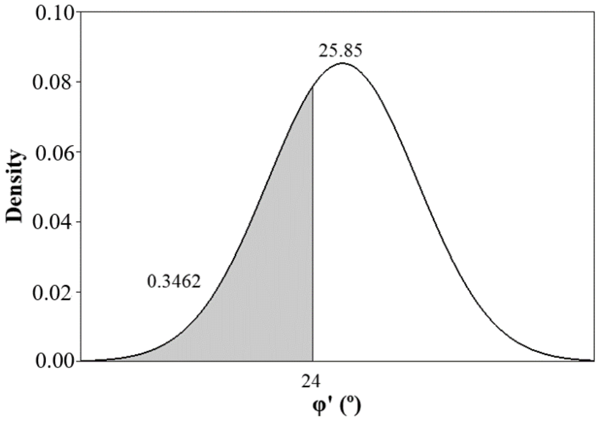

Figure 12. Comparison of the effective friction angle from CPTu and triaxial tests.

In complement of the comparison with the triaxial tests, the results herein were compared with the dataset shown by Ouyang & Mayne (2019). The red dots in Figure 13 shows the results considering the mean (φ'_{CPTu} = 26º) and the 35th percentile ($\varphi'_{CPTu\text{-}P35}$ = 24º) of the CPTu distribution plotted against the value determined using the triaxial compression test (φ'_{txc} = 24º). As can be seen, the mean value reached the lower boundary of the authors dataset while the 35th percentile almost reached the trendline of the equation proposed by the authors.

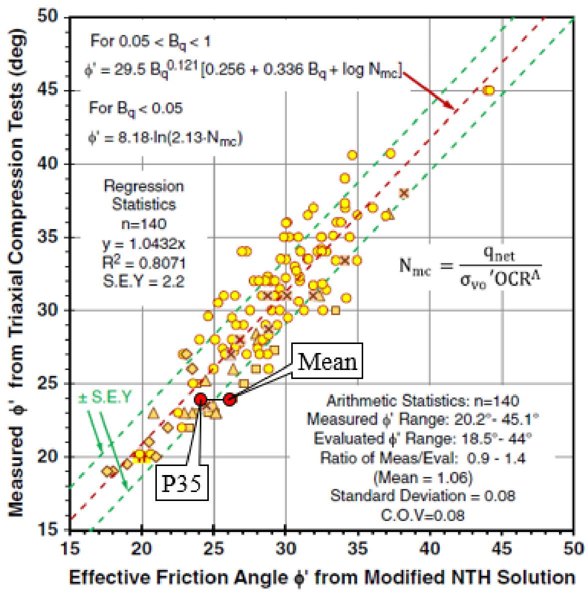

Figure 13. Comparison of effective friction angle from the stiff clay analysed and Ouyang & Mayne (2019) results.

5. Conclusion

This paper presented a case study to evaluate the behaviour and the effective friction angle of a Brazilian stiff dilative clay using laboratory and field tests. Also, geotechnical characterization was conducted by laboratory tests (grain-size distribution, Atterberg Limits, and specific gravity of soil). The behaviour-based classification showed that the evaluated material was predominantly clay-like and presented a dilative behaviour at large strain. Furthermore, the same behaviour observed in the dissipation tests performed during the CPTu. Additionally, the in-situ classification was consistent with the textural classification assessed by the laboratory data and the stress-strain behaviour observed in the triaxial compression tests.

Given that the stiff clay presented a dilative behaviour under shear, the effective friction angle was determined using the triaxial compression test and the CPTu, using the methodology proposed by Ouyang & Mayne (2019). The effective friction angle determined using the triaxial compression was φ'_{txc} = 24º, which corresponded to the 35th percentile of the data determined using the CPTu. This indicates that 65% of the in-situ effective friction angle data obtained by the modified NTH methodology is higher than the laboratory measurement. However, this difference may be related to the natural dispersion of the parameter or factors such as: i) the mineralogy; ii) the natural variation of the cone resistance; and iii) the porepressure profiles, as already observed by Ouyang & Mayne (2018, 2019).

Finally, it is important to highlight that conclusions obtained in this paper are specific to the brazilian stiff clay studied and the authors do not recommend a direct replication of the results presented herein without a proper study, especially when applied to guide the design parameters of a geotechnical project.

Acknowledgments

The authors would like to acknowledge the support received by Pimenta de Ávila for the paper development.

References

American Society for Testing and Materials – ASTM. 2007. D422-63: Standard Test Method for Particle-Size Analysis of Soils.

American Society for Testing and Materials – ASTM. 2018. D4318-17e1: Standard Test Methods for Liquid Limit, Plastic Limit, and Plasticity Index of Soils.

American Society for Testing and Materials – ASTM. 2020. D4767-11: Standard Test Method for Consolidated Undrained Triaxial Compression Test for Cohesive Soils.

American Society for Testing and Materials – ASTM. 2020. D792-20: Standard Test Methods for Density and Specific Gravity (Relative Density) of Plastics by Displacement.

Assis, A. P. 2020. Risk management for geotechnical structures: consolidating theory into practice. Soil and Rocks, 43(3), 311-336.

Castro, G. 1969. “Liquefaction of sands”. Ph. D. Thesis, Harvard University, Mass.

Chen, B. S., & Mayne, P. W. 1996. “Statistical relationships between piezocone measurements and stress history of clays”. Canadian Geotechnical Journal, 33(3), 488-498.

International Organization for Standardization - ISO 22476-1. 2022: Geotechnical investigation and testing — Field testing — Part 1: Electrical cone and piezocone penetration test.

Kulhawy, F. H., & Mayne, P. W. 1990. Manual on estimating soil properties for foundation design (No. EPRI-EL-6800). Electric Power Research Inst., Palo Alto, CA (USA); Cornell Univ., Ithaca, NY (USA). Geotechnical Engineering Group.

Lunne, T.; Robertson, P.K. & Powell, J.J.M. 1997. "Cone Penetration Testing in Geotechnical Practice". First Edition. Abingdon: E & FNSpon Press.

Lade, P.V. 2016. "Triaxial testing of soils". John Wiley & Sons, Ltd, Chichester, U.K.402 p.

Mayne P. W. et al.., 2023 "A CPT design parameter manual." ConeTec.

Ouyang, Z., & Mayne, P. W. 2018. "Effective friction angle of clays and silts from piezocone penetration tests". Canadian Geotechnical Journal, 55(9), 1230-1247.

Ouyang, Zhongkun; Mayne, Paul W. 2019. "Modified NTH method for assessing effective friction angle of normally consolidated and overconsolidated clays from piezocone tests". Journal of Geotechnical and Geoenvironmental Engineering, v. 145, n. 10, p. 04019067.

Robertson, P. K., & Campanella, R. G. 1983. "Interpretation of cone penetration tests. Part I: Sand." Canadian geotechnical journal, 20(4), 718-733.

Robertson, P. K. 2009. Interpretation of cone penetration tests - A unified approach." Can. Geotech. J. 46 (11): 1337–1355. https://doi.org/10.1139/T09-06510.1139/T09-065.

Robertson, P. K. 2016. "Cone Penetration Test (CPT)-based soil behaviour type (SBTn) classification system—an update." Canadian geotechnical journal, 53(12), 1910-1927.

Schneider, J.A., Randolph, M.F., Mayne, P.W., and Ramsey, N.R. 2008. Analysis of factors influencing soil classification using normalized piezocone tip resistance and pore pressure parameters. Journal of Geotechnical and Geoenvironmental Engineering, ASCE, 134(11): 1569–1586. doi:10.1061/(ASCE)1090-0241(2008)134:11(1569).

Schnaid, F. 2009. In situ testing in geomechanics: the main tests. CRC Press.

Senneset, K., R. Sandven, and N. Janbu. 1989. "Evaluation of soil parameters from piezocone tests." Transp. Res. Rec. 1235: 24–37.

Song, C., Bekele, B., & Silvey, A. 2019. "Pore pressure responses of overconsolidated soils in a partially drained piezocone penetration test". Journal of Engineering Mechanics, 145(4), 04019017.

Uzielli, M., & Mayne, P. W. 2019. "Probabilistic assignment of effective friction angles of sands and silty sands from CPT using quantile regression". Georisk: Assessment and Management of Risk for Engineered Systems and Geohazards, 13(4), 271-275.